Middle Atmosphere Simulated with High Vertical and Horizontal Resolution Versions of a GCM: Improvements in the Cold Pole Bias and Generation of a QBO-like Oscillation in the Tropics

KEVIN HAMILTON, R. JOHN WILSON, AND RICHARD S. HEMLER

NOAA/Geophysical Fluid Dynamics Laboratory, Princeton University, Princeton, New Jersey

(Manuscript received 27 August 1998, in final form 22 February 1999)

ABSTRACT

The large-scale circulation in the Geophysical Fluid Dynamics Laboratory ''SKYHI'' troposphere–stratosphere–mesosphere finite-difference general circulation model is examined as a function of vertical and horizontal resolution. The experiments examined include one with horizontal grid spacing of ~35 km and another with ~100 km horizontal grid spacing but very high vertical resolution (160 levels between the ground and about 85 km). The simulation of the middle-atmospheric zonal-mean winds and temperatures in the extratropics is found to be very sensitive to horizontal resolution. For example, in the early Southern Hemisphere winter the South Pole near 1 mb in the model is colder than observed, but the bias is reduced with improved horizontal resolution (from ~70°C in a version with ~300 km grid spacing to less than 10°C in the ~35 km version). The extratropical simulation is found to be only slightly affected by enhancements of the vertical resolution. By contrast, the tropical middle-atmospheric simulation is extremely dependent on the vertical resolution employed. With level spacing in the lower stratosphere ~1.5 km, the lower stratospheric zonal-mean zonal winds in the equatorial region are nearly constant in time. When the vertical resolution is doubled, the simulated stratospheric zonal winds exhibit a strong equatorially centered oscillation with downward propagation of the wind reversals and with formation of strong vertical shear layers. This appears to be a spontaneous internally generated oscillation and closely resembles the observed QBO in many respects, although the simulated oscillation has a period less than half that of the real QBO.

1. Introduction

Global general circulation models (GCMs) have had some success in simulating the circulation in the stratosphere and mesosphere (see Hamilton 1996 for a review). However, there are two important deficiencies that affect the middle-atmospheric circulation in most current GCMs. First, there is a tendency for the circulation in the extratropics to be unrealistically close to radiative equilibrium, notably with simulated winter polar temperatures in the stratosphere being much colder than observed. In models the eddy fluxes do drive an overturning circulation that results in a dynamical warming of the winter pole, but the eddy activity is apparently too weak to produce a realistic temperature structure. This problem can, of course, be alleviated by the inclusion of some additional source of drag on the zonal-mean wind (e.g., Hamilton 1995, 1997). This extra drag may take the form of a parameterization of anticipated subgrid-scale gravity wave effects (e.g., Manzini et al. 1997; McFarlane et al. 1997; Medvedev et al. 1998), but such parameterizations cannot at present be derived from first principles. The second major problem is that the tropical stratospheric circulation in most models has unrealistically weak interannual variability, notably an absence of the quasi-biennial oscillation (QBO), which is such a dominant aspect of the circulation in this region of the real atmosphere. These two issues represent major obstacles to the goal of constructing a general circulation model of the middle atmosphere that can be used for credible chemistry and climate perturbation experiments.

Recent studies have shown that both the extratropical and tropical simulation in at least some middle-atmospheric GCMs can be strongly affected by the spatial grid resolution employed. In particular, it appears that the cold winter pole problem improves with finer horizontal model resolution (Mahlman and Umscheid 1987; Boville 1995; Hamilton et al. 1995). Hamilton et al. (1995, hereafter HWMU) discussed multiyear simulations with versions of the Geophysical Fluid Dynamics Laboratory (GFDL) SKYHI troposphere–stratosphere–mesosphere GCM using 3°–3.6°, 2°–2.4°, and 1°–1.2° latitude–longitude grid spacing. At 3° grid spacing the Southern Hemisphere (SH) winter mean polar temper-

Corresponding author address: Dr. Kevin Hamilton, NOAA/GFDL, Princeton University, P.O. Box 308, Princeton, NJ 08542.
E-mail: kph@gfdl.gov

atures near 1 mb are ~70°C colder than observed, while the bias is reduced to less than 35°C in the 1° model. A similar, though less dramatic, effect is apparent in the Northern Hemisphere (NH) winter simulations reported in HWMU. Jones et al. (1997) showed that the improvement in the SH winter circulation continued when the SKYHI grid spacing was reduced still further to 0.6°–0.72°. Boville (1991, 1995) demonstrated somewhat similar results for simulations made with the middle-atmospheric version of the National Center for Atmospheric Research (NCAR) spectral Community Climate Model with horizontal resolutions varying from T31 to T106. It appears that when a GCM is run with higher horizontal resolution the model generates stronger wave fluxes, which then act to drive the zonal-mean circulation farther from radiative equilibrium.

The issue of how vertical resolution affects the simulation produced by middle-atmospheric GCMs appears not to have been addressed as systematically, but there have been some relevant studies that have demonstrated important effects, notably in the Tropics. Boville and Randel (1992) used a T21 version of the NCAR GCM to examine the dependence of simulations on the vertical resolution employed. As they reduced vertical level spacing from ~2.8 to ~0.7 km, Boville and Randel found little effect on the extratropical circulation but did discover that the strength of the easterly phase of the semiannual oscillation near the equatorial stratopause increased substantially. More recently Takahashi (1996) reported that in a version of the Japanese Center for Climate System Research (CCSR) spectral GCM, the stratospheric mean wind undergoes a large-amplitude oscillation with period ~1.4 yr when the vertical level spacing in the lower stratosphere is reduced to about 700 m. This appears to be the first report in a GCM of a QBO-like interannual oscillation of realistic amplitude. Horinouchi and Yoden (1998) found a similar QBO-like oscillation in a somewhat idealized version of another spectral GCM. In both the Takahashi (1996) and Horinouchi and Yoden (1998) models it is necessary to employ vertical level spacing somewhat less than 1 km for the QBO-like oscillations to occur.

This paper will describe initial results obtained with the GFDL SKYHI GCM in several new versions with very fine horizontal and vertical grid spacing. The baseline result will be an integration at the highest resolution control simulation discussed in HWMU, that is, 1°–1.2° horizontal grid spacing and 40 levels between the ground and ~80 km. Simulations with twofold and fourfold enhancement of this vertical resolution and another simulation with a threefold enhancement of the horizontal resolution will be described here. The present paper will give a preliminary description of only the zonal-mean aspects of the middle-atmospheric simulation, providing a context for more detailed analysis of the results to be presented in later publications.

The model and the integrations considered here are described in section 2. Basic results for the extratropical zonal-mean circulation are discussed in section 3. Section 4 considers the results in the Tropics in the high vertical resolution control simulation and in another experiment with the same model, but employing perpetual equinox solar insolation. Results are discussed in more detail and conclusions are summarized in section 5.

2. The SKYHI model formulation and the control integrations

The SKYHI model (Fels et al. 1980; HWMU) solves the primitive equations on a latitude–longitude nonstaggered grid using second-order horizontal differencing. Zonal Fourier filtering of fields poleward of about 50° latitude is used to maintain a roughly isotropic horizontal resolution. The SKYHI model uses a hybrid vertical coordinate that is terrain-following near the ground, merging gradually into pure isobaric coordinates above 353 mb. The various latitude–longitude grid spacings referred to in this paper are denoted N30 (3°–3.6°), N90 (1°–1.2°), N150 (0.6°–0.72°), and N270 (0.333°–0.4°), where the N notation refers to the number of grid rows between the pole and equator. The three vertical grid spacings considered are L40, L80, and L160, where the L notation denotes the number of full model levels. The distribution of levels for each resolution is shown in Fig. 1. The L40 grid spacing is the same as that employed in HWMU and other SKYHI publications and stretches from the ground to the top full level at 0.0096 mb. The L80 level structure represents an almost uniform doubling of the L40 vertical grid spacing at all heights. The L160 grid is nearly a uniform doubling of the L80 grid, but the top full level is located a few km higher (0.0052 mb). In the lower stratosphere the level spacing is very roughly 1.6, 0.8, and 0.4 km for the L40, L80, and L160 grids, respectively.

The upper boundary condition is such that the vertical velocity is required to vanish at a half-level formally located at zero pressure. In order to reduce reflection of vertically propagating waves from the model top, a linear damping of the deviation from the zonal mean is applied to the temperature and horizontal wind near the top of the model. In the L40 versions this extra drag acts only at the highest model full level (0.0096 mb) with a timescale of 10 800 s. In the L80 version the drag acts on the top two levels (with timescales of 7200 and 21 400 s), and in the L160 it is applied at the top four levels (7200, 10 800, 21 400, 86 400 s).

Radiative and other subgrid-scale mixing parameterizations are discussed in HWMU and references therein. The only change affecting some of the integrations reported here concerns the treatment of the surface heat balance over land. The ''old'' scheme involves a simple energy balance at the earth's surface (i.e., no thermal inertia in the surface) and is the same as in the N90 model described in HWMU. In the ''new'' scheme the thermal inertia of the soil is taken into account and prognostic equations for the temperatures of two soil

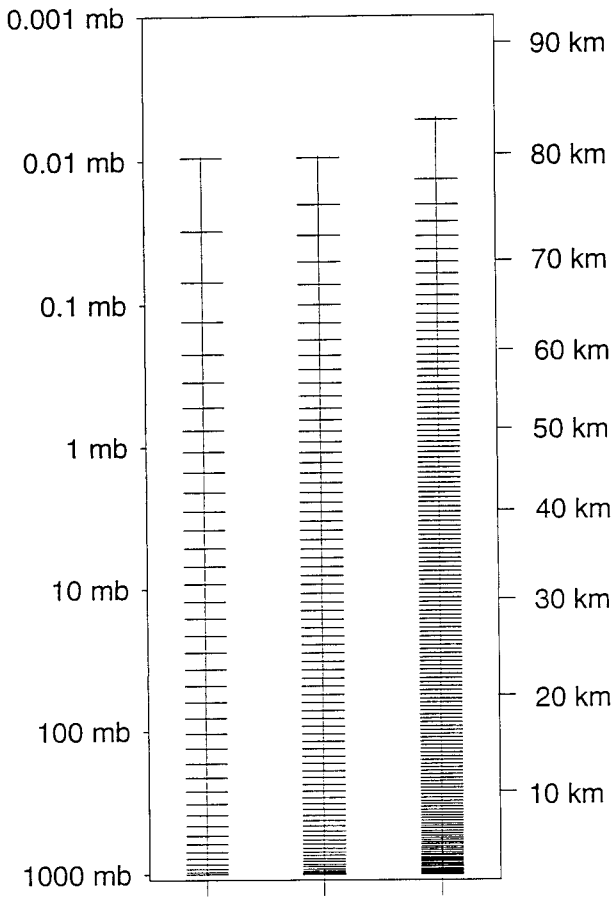

FIG. 1. The three different numerical model level structures discussed in this paper: L40 (left), L80 (center), and L160 (right). The pressures for the levels shown are for a surface pressure of 1013 mb. The heights given on the right axis are for the midlatitude spring–fall *U.S. Standard Atmosphere.*

levels are included (the thickness of the top level is taken to be 0.05 m).

No parameterization of subgrid-scale gravity wave effects is included in any of the model integrations discussed here. The vertical and horizontal diffusion parameterizations have coefficients that scale with the vertical and horizontal grid spacing, respectively (see Levy et al. 1982; Andrews et al. 1983).

The ozone mixing ratios are specified in the manner outlined in Fels et al. (1980). The prescribed values are somewhat idealized (notably in having no interhemispheric asymmetry). They also take no account of post-1980 observations and thus do not reflect the presence of the ozone hole phenomenon. All the detailed comparisons with observations that will be presented here will employ only measurements before 1985.

In all integrations the surface temperatures over ocean points are specified as a function of time of year. The climatological values used are identical to those employed in HWMU. Table 1 summarizes the various integrations discussed here. The N90L40 integration is a continuation of that described in HWMU. The 10-yr N30L40 experiment was initialized from results taken from the long integration of an earlier version of the model described in HWMU. The higher-resolution integrations were all initialized using fields interpolated from the 5 May results of the second year of the N90L40 model run. In all cases the results for the first 5–31 May period were discarded and analysis starts with the June results.

TABLE 1. Summary of the control integrations discussed in this paper.

Resolution	Length of integration available for analysis	Notes
N30L40	10 yr	
N90L40	2 yr	surface heat balance
N150L40	June	
N90L80	2 yr	356 ppmv CO_2
N270L40	June–December	
N90L160	June	356 ppmv CO_2

The longwave radiative transfer for CO_2 in the model is handled with the method of Fels and Schwarzkopf (1981), which employs transmission functions interpolated from standard values for different standard temperature profiles. The L40 integrations were performed with prescribed CO_2 mixing ratio of 330 ppmv, but the L80 and L160 integrations employed 356 ppmv. This ~8% difference might be expected to affect stratospheric temperatures by ~1°C, since a doubling of CO_2 is expected to produce stratospheric cooling of up to ~10°C (e.g., Fels et al. 1980). After the integrations described here were completed, it was discovered that the L80 and L160 models were run with standard temperature profiles that in the mesosphere were inconsistent with the standard transmission functions. This causes overestimates of the longwave cooling in the mesosphere, although this becomes significant only above about 0.03 mb. At the 0.01-mb level this may result in a spurious cold bias of as much as ~10°C.

3. Results for the extratropics in the control integrations

The focus here is on the austral winter and spring seasons since the relatively small interannual variations during this time of year may allow conclusions to be drawn from the short records available from the high-resolution simulations. The SH winter is also the season in which earlier GCM simulations of the stratosphere have been most significantly in error (e.g., HWMU; Boville 1995). Figure 2 shows the zonal-mean zonal wind for each of June, July, and August for the N90L40, N90L80, and N270L40 integrations. The N90L40 and N90L80 results represent a two-year mean ''climatology'' while just a single month is used for the N270 results depicted. In the SH extratropics the N90L40 results display almost exactly the same biases that have

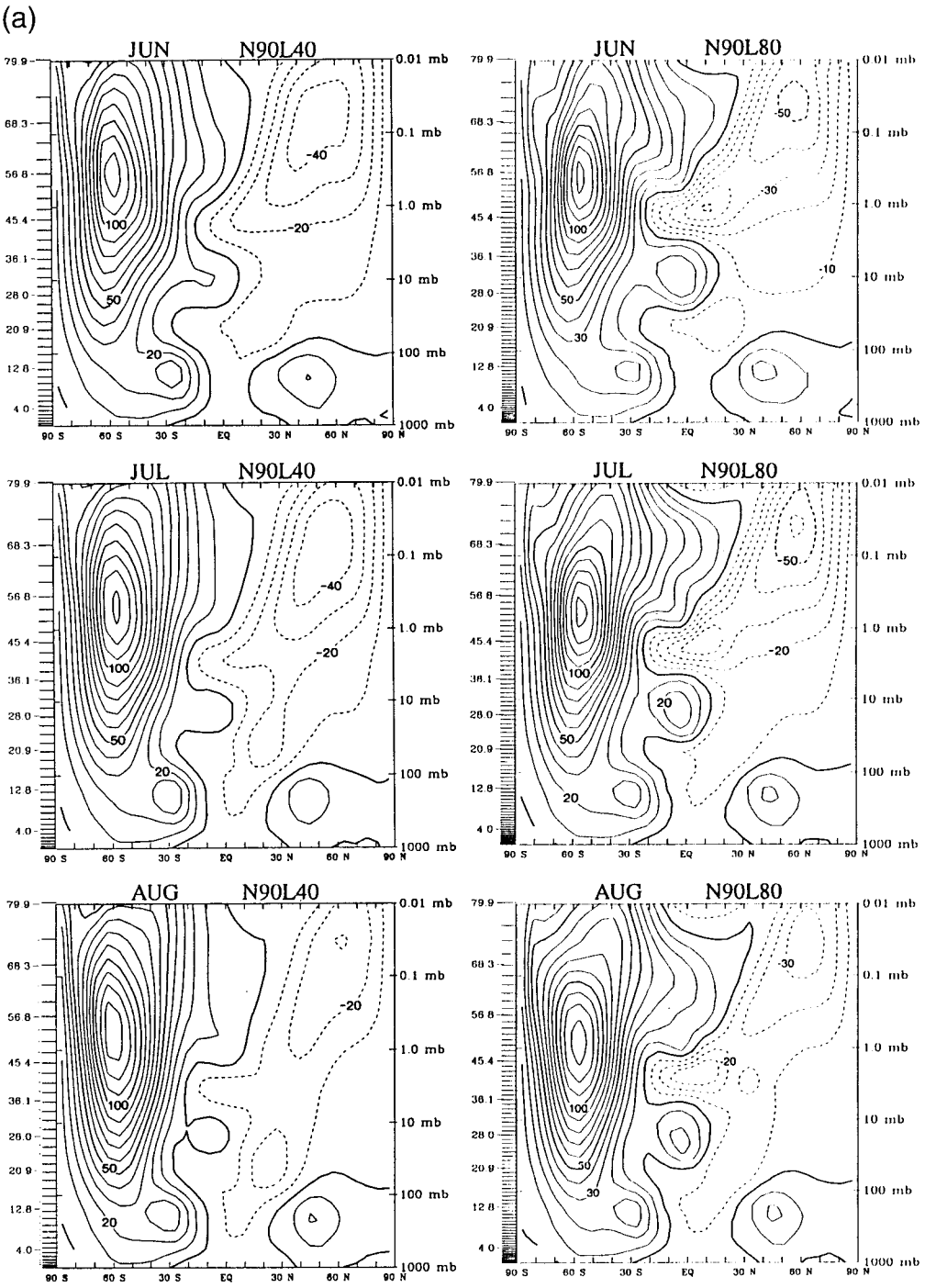

FIG. 2. The zonal-mean zonal wind for the individual months: June (top), July (middle), and August (bottom), in the N90L40 (left), N90L80 (middle), and N270L40 (right) experiments. The contour interval is 10 m s^{-1} and easterly winds are denoted by dashed contours. Results represent 2-yr means for the N90L40 and N90L80 inte-

been documented for earlier N90L40 runs in HWMU and Hamilton (1995). As expected, the polar night jet in each month is stronger than observed (e.g., as seen in climatologies of Barnett and Corney 1985; Wu et al. 1987; Fleming et al. 1988; Randel 1992) and the vortex is too tightly confined near the pole. Thus, for example, the peak zonal-mean wind in the July N90L40 simulation is over 130 m s^{-1} and occurs near 0.5 mb and 60°S. The corresponding jet peak in the July climatology of Fleming et al. (1988) is 90 m s^{-1} and is located nearer

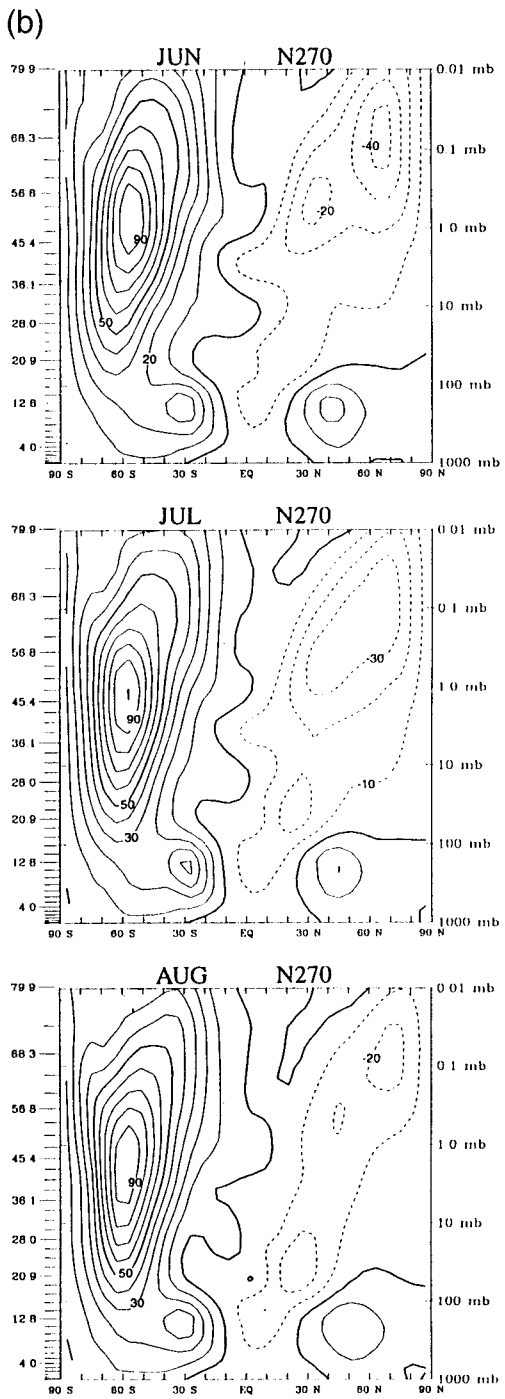

FIG. 2. (*Continued*) grations and just a single year for N270L40. The standard heights for selected pressures are given in km on the left axis of each panel.

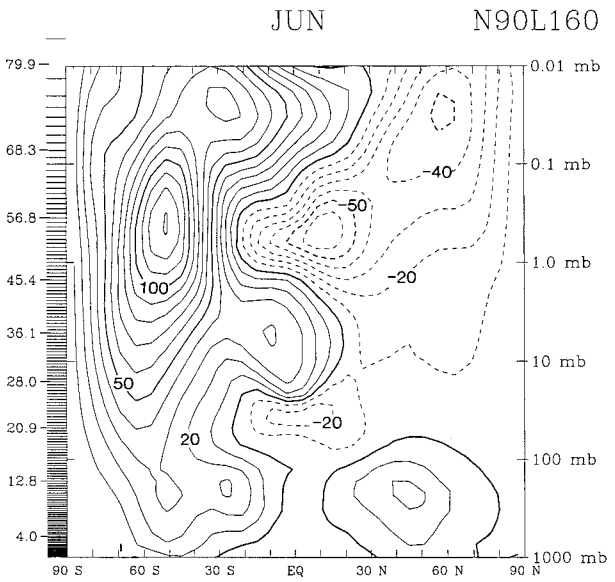

FIG. 3. The zonal-mean zonal wind for a single June in the N90L160 model integration. The contour interval is 10 m s^{-1} and easterly winds are denoted by dashed contours.

40°S. The N90L80 results in the extratropics are very similar to those for the N90L40 simulations. The zonal-mean zonal winds for the single June of the N90L160 simulation are shown in Fig. 3. In the extratropics the results are very similar to the N90L40 and N90L80 simulation. By contrast, the N270L40 wind structure in the SH extratropics seen in Fig. 2 is significantly improved over the lower-resolution results in each of June, July, and August. The peak polar night jet speeds are reduced by 30–40 m s^{-1} below those in any of the N90 results, and the N270 simulated vortex edge has a clear equatorward tilt with height, in qualitative agreement with observations. However, even at the N270 resolution, the slope of the vortex edge is not as pronounced as in observations, and the vortex in the upper stratosphere and mesosphere is still somewhat too tightly confined to high latitudes.

Figures 2 and 3 also show that the winds in the extratropical summer hemisphere are more strongly affected by the change in horizontal resolution from N90 to N270 than the increase in vertical resolution from L40 to L80 or L160. In each month the summertime easterlies in the mesosphere are somewhat weaker in the N270 simulation relative to the N90 simulations. The N270 simulation appears to be more realistic in this regard, particularly in having the jet peak at a somewhat lower altitude than in the N90 simulations.

Figure 4 shows the zonal-mean temperature biases relative to the Fleming et al. (1988) climatology for June, July, and August for the same simulations as in Fig. 2. The deficiencies in the model polar vortex apparent in Fig. 2 are reflected in the temperature biases. The N90L40 simulation has a cold bias concentrated in the high southern latitudes of the upper stratosphere and lower mesosphere that exceeds 30°C in June, 45°C in July, and 55°C in August. These biases are reduced only slightly in the N90L80 model but are substantially alleviated in the N270 simulation.

There is a global-mean cold bias in the upper stratosphere of the order of 5°C that appears in each month

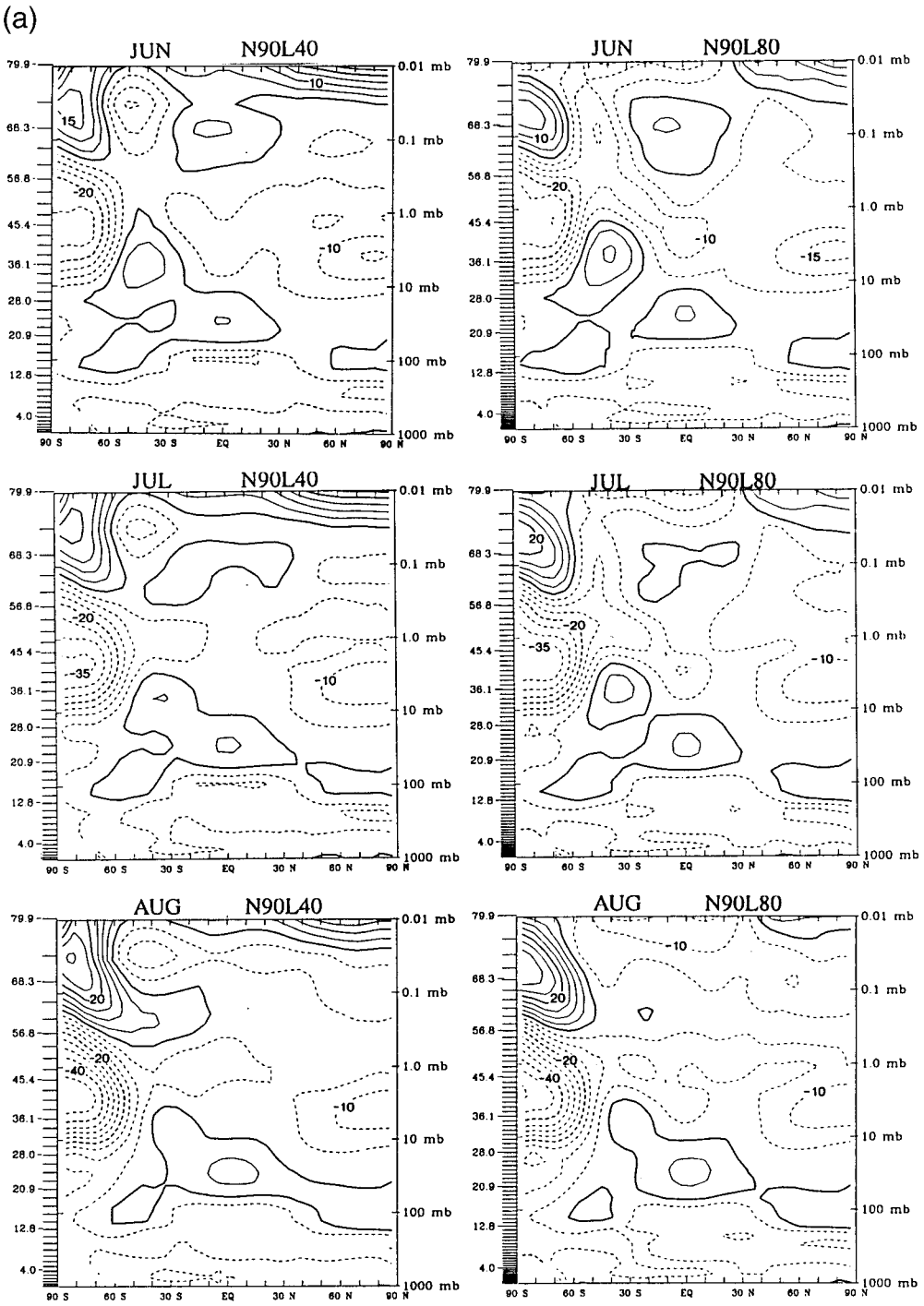

FIG. 4. As in Fig. 2, but for the difference in the simulated zonal-mean temperature from the observed climatology of Fleming et al. (1988). The contour interval is 5°C and dashed contours denote regions where the SKYHI simulation is colder than the observed climatology.

in each simulation. This bias could be eliminated by changing the prescribed ozone concentrations within the bounds of current observational uncertainty (Orris 1997). Above ~0.03 mb there are lower global-mean temperatures in the N90L80 simulation than in either of the L40 simulations. This is at least partly attributable to the error in the L80 transmission functions described in section 2.

The effects of horizontal resolution changes on simulated SH high-latitude temperatures in June are sum-

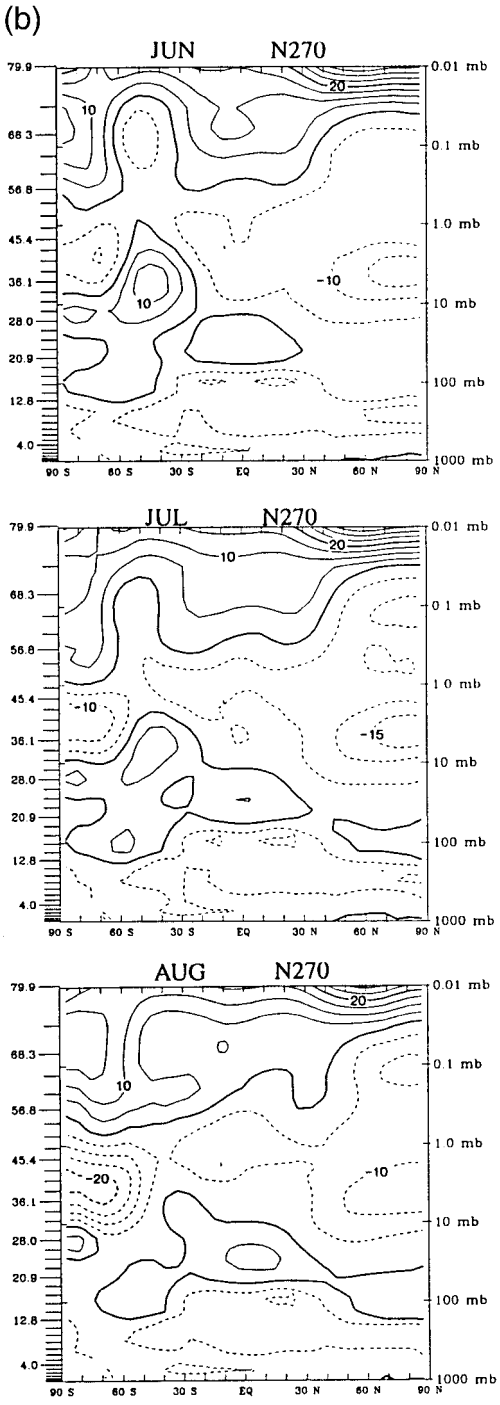

FIG. 4. (*Continued*)

marized in Fig. 5. This shows the zonal-mean temperatures at 70°S for the single N270 June, the single N150L40 June, and three individual N90L40 Junes: two from the control run and a third from the short (March–June) integration of the same model described in Jones et al. (1997). Also displayed is a 10-yr mean June climatology for the N30L40 integration. These model results are compared with the observed climatology of Fleming et al. (1988). The N30 simulation is affected by a strong cold bias that exceeds 50°C near 1 mb. The N90 simulations represent a very substantial improvement over the N30 result, with the cold bias at most stratospheric levels reduced by more than half. The improvement in simulated temperatures with resolution continues with the N150 and the N270 models. In fact, in the N270 simulation the cold bias in June is largely eliminated. It is certainly possible that further reductions in horizontal grid spacing in SKYHI could lead to SH winter polar temperatures that are actually warmer than observed. In fact, near 20 mb the N270 simulation is already somewhat warmer than the Fleming et al. climatology in June, July, and August (Figs. 4 and 5).

As one might expect, the changes in mean temperature with model resolution reflect changes in the large-scale circulation in the middle atmosphere. Figure 6 compares the transformed Eulerian pressure velocity, $\overline{\omega}^*$ (e.g., Andrews et al. 1983, 1987), averaged over the N270 June and each of three N90L40 Junes. The results for the N90 model are somewhat noisy since the averages are based on once-per-day instantaneous snapshots (much more frequent averaging was used for the data archived in the N270 run). The result does clearly show stronger mean downwelling in the N270 model poleward of about 50° in the winter hemisphere (recall that the pressure velocity is generally positive for downwelling). This is compensated by stronger rising motion in the summer hemisphere. Similar results are found at lower levels in the stratosphere (not shown). All of these results fit into a consistent and expected picture; that is, as resolution is improved there is more wave drag on the flow, resulting in an increased strength in the pole-to-pole overturning circulation and higher (lower) temperatures in the high-latitude winter (summer) high latitudes. The effects on the tropical mean circulation are harder to anticipate as the mean meridional circulation at low latitudes is not so simply related to the eddy mean flow driving (Haynes et al. 1991). The results in Fig. 6 suggest the possibility of a somewhat complicated change in the pattern of tropical upwelling, but the magnitude of the change at low latitudes is so small that it is hard to clearly discern above the interannual and sampling noise.

Figure 7 compares the 70°S June temperatures for the N90 models with different vertical resolutions. Results are shown again for the three N90L40 realizations, two Junes for the N90L80 model, and the single available N90L160 June. Over most of the height range shown the results for the different resolutions are quite similar, although there may be a significant difference just below ~0.1 mb where the L160 model has its stratopause slightly lower than the other models. Deviations of more than ~5°C are limited to the region above ~0.03 mb, where the colder L80 and L160 results are certainly

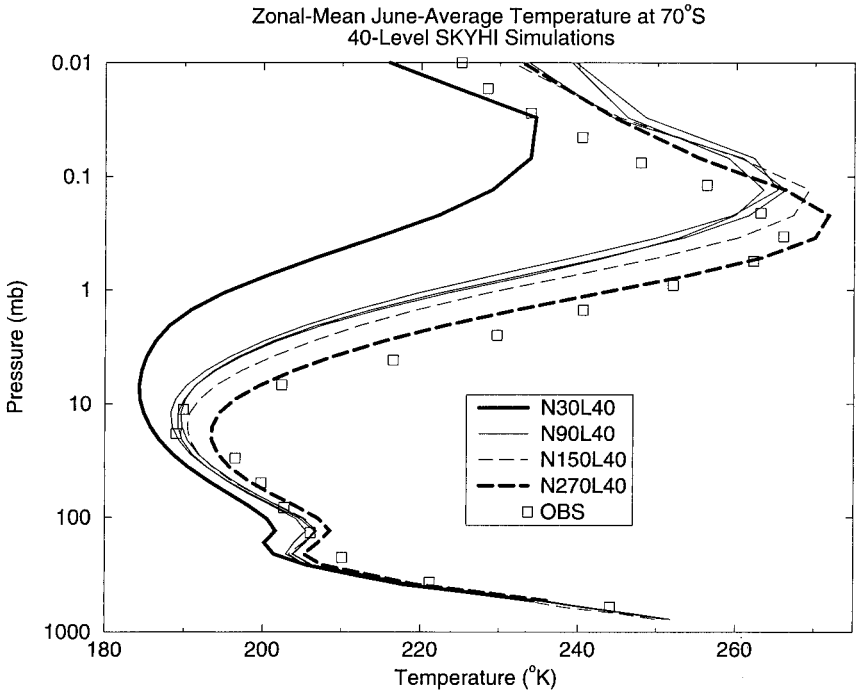

FIG. 5. The June average, zonal-mean temperature at 70°S for several different L40 SKYHI experiments and for the observed climatology of Fleming et al. (1988). Results for three individual Junes are shown for the N90L40 model. The heavy solid curve represents the June climatology in a 10-yr integration of an N30L40 version.

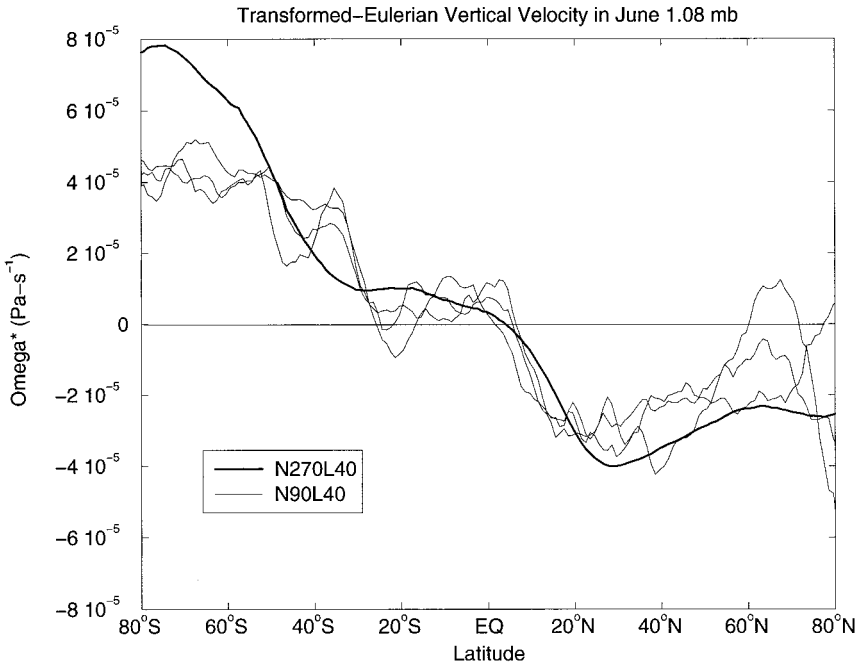

FIG. 6. The June average, zonal-mean transformed Eulerian pressure velocity, $\overline{\omega}^*$, at the 1.08-mb level from the N270L40 integration and from three individual years of the N90L40 model simulation. A 10° running mean has been applied to reduce sampling noise.

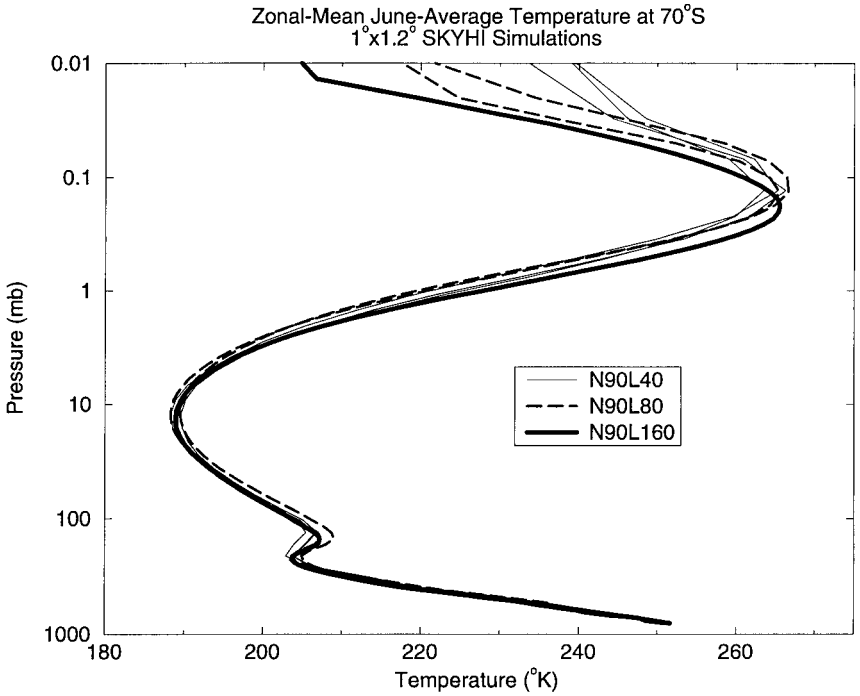

FIG. 7. The June average, zonal-mean temperature at 70°S for several different N90 SKYHI experiments. Results for two individual Junes are shown for the N90L40 and N90L80 cases and for the single June in the N90L160 integration.

contaminated by the error in the CO_2 transmission function described in section 2.

Figures 8 and 9 present the monthly zonal wind and temperature results for each of September, October, and November for the N90L40, N90L80, and N270L40 simulations. In each model the magnitude of SH winter polar temperature bias peaks in September, and the cold bias is reflected in unrealistic simulation of the zonal-mean wind structure. Once again, however, the bias depends strongly on the horizontal resolution, exceeding 60°C near 3 mb in the N90L40 and N90L80 models, but being less than 40°C in the N270 model. In October and then again in November the magnitude of the peak SH polar cold bias is reduced in all the models, and the height at which the peak cold bias occurs also drops. The first signs of the cold bias in the NH polar region appear in October, and this bias intensifies in November. In the N90L40 simulation the 1-mb North Pole temperature is ~25°C too low in October and ~40°C too low in November. These biases are reduced somewhat in the N90L80 model, but the reduction is much more substantial in the N270 version.

A symptom of the problems with the simulation of the SH spring stratospheric circulation in GCMs has been the tendency for unrealistically late SH final warmings. For example, Mahlman et al. (1994) show that the N30L40 SKYHI simulation still maintains a quite intact SH polar vortex at the end of November. The present N270 model has produced a simulation very much improved in this regard. Figure 10 shows the evolution of the zonal-mean zonal wind at 10 mb in the N270 simulation during the SH spring compared with an observed composite based on 6 yr of National Centers for Environmental Prediction global analyses (adapted from Farrara and Mechoso 1986). The overall development of the final breakup of the vortex in the model is quite realistic, with the deceleration of the zonal-mean westerlies occurring first at low latitudes and appearing to propagate poleward. The strength of the peak mean wind decelerations are also comparable in the model and observations. However, the whole warming process in the model is delayed by about two weeks, consistent with the documented model cold bias at high SH latitudes throughout the spring. Figure 11 shows the height–time evolution of the zonal-mean temperature at high southern latitudes during the springtime in the N270 simulation. It can be compared with the observational composite in Fig. 3 of Farrara and Mechoso (1986). The general pattern of a downward-propagating warming is common to the simulation and observations, but once again the model warming is seen to be delayed by about two weeks relative to that observed.

Figure 12 shows the zonal-mean temperature at 70°S and 70°N in each individual January of the N90L40 and N90L80 experiments and compares these with the Fleming et al. climatology. At 70°S the results for the different model resolutions are very close everywhere except right near 0.01 mb, where they are affected by the

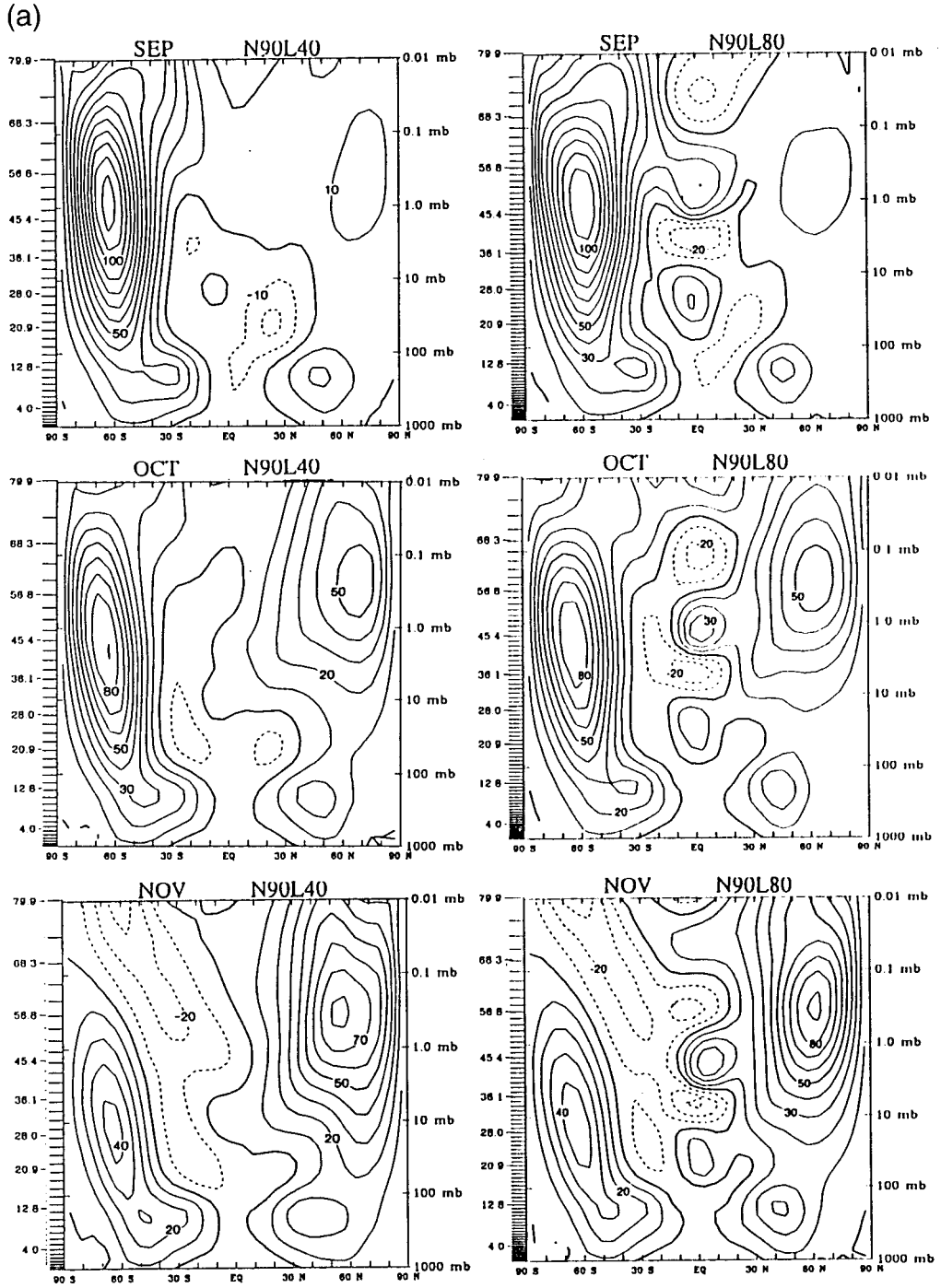

FIG. 8. As in Fig. 2, but for September, October, and November.

transmission function error. Interestingly, the results for both models show a significant cold bias near the tropopause. This bias in the high-latitude summer tropopause is also seen in NH summer (e.g., Fig. 4) in these SKYHI integrations and has also been found in other GCMs (e.g., Boville 1995). At 70°N there is enough interannual variability apparent in both models that it is difficult to draw conclusions about the effect of the resolution on the simulation. Figure 13 shows a similar comparison of N90L40 and N90L80 temperatures in April. Again at 70°S there seems to be little difference between the L40 and L80 results except above 0.3 mb.

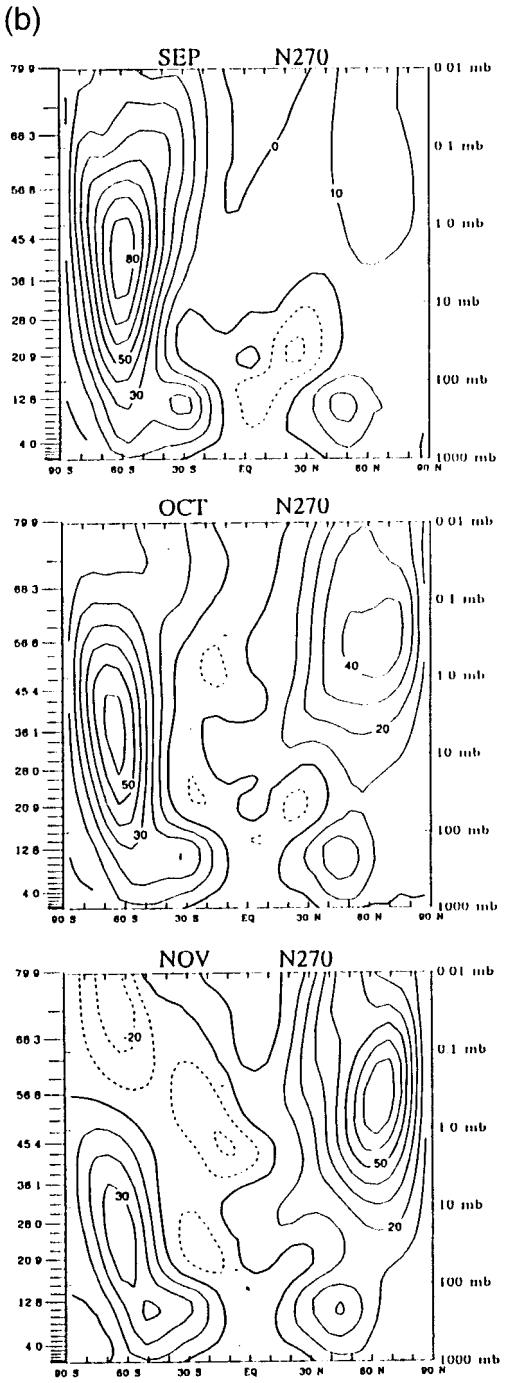

FIG. 8. (*Continued*)

At 70°N any systematic difference between L40 and L80 results appears to be buried within the strong interannual variability.

4. Tropical wind variability

Near the equator the zonal-mean winds in the L80 and L160 experiments are dramatically different from those in any of the L40 simulations. The presence of strong easterly and westerly jets centered on or near the equator is quite apparent in the wind cross sections for the high vertical resolution simulations shown in Figs. 2, 3, and 8. The top two panels of Fig. 14 compare the height–time evolution of the equatorial zonal-mean zonal wind in the N90L40 and N90L80 simulations. In the L40 model the winds near the stratopause undergo a semiannual oscillation with somewhat realistic features, but the winds in the tropical lower stratosphere are nearly constant (typical behavior in most GCMs). The middle panel of this figure shows the equatorial wind in the 80-level version of the model. The equatorial winds and the vertical shears are much stronger in the L80 model. Above about 1 mb the semiannual variation still dominates, but in the lower and middle stratosphere a longer period oscillation is evident. The mean wind evolution in the lower and middle stratosphere displays both the downward propagation of wind regimes and the concentration of vertical shear into narrow zones that are characteristic of the QBO in the real atmosphere. However, the period of the wind oscillation appears to be about one year, which, of course, is much shorter than that of the real QBO. From the limited two-year simulation available, it is not clear whether the period of the lower stratospheric wind variations is exactly one year.

The N90L80 model was rerun for two years (starting from initial conditions taken from the first March of the seasonally varying control) with fixed equinoctial (22 March) solar insolation and sea surface temperatures. The result for the equatorial zonal-mean zonal wind is shown in the lower panel of Fig. 14. The mean wind evolution in the lower and middle stratosphere can be seen to be quite similar to that in the seasonally varying run, showing that this oscillation is indeed a spontaneous ''QBO-like'' variation, rather than being forced by the annual cycle. It is interesting that the QBO-like oscillation reported in other GCMs or simplified GCMs also have periods considerably shorter than the real QBO: 1.4 yr in the GCM of Takahashi (1996), and 1.1 yr in the model of Horinouchi and Yoden (1998). Horinouchi and Yoden (1998) speculated that their unrealistically short period might be due to too-weak tropical mean upwelling. This is certainly a possibility in the present model as well.

The peak shears in the zonal-mean zonal wind in the tropical stratosphere in the L80 simulations are ~0.01–0.02 s^{-1}, values that are comparable to those actually seen in the monthly mean in single station observations (e.g., Naujokat 1986). The largest westerly shears in the simulation are significantly stronger than the largest easterly shears, again in agreement with observations. The meridional structure of the oscillation also appears to be fairly realistic, with the equatorially centered jets in Figs. 2 and 8 that can be characterized as having roughly Gaussian shape with meridional width ~15° (e.g., Newell et al. 1974; Belmont et al. 1974). The

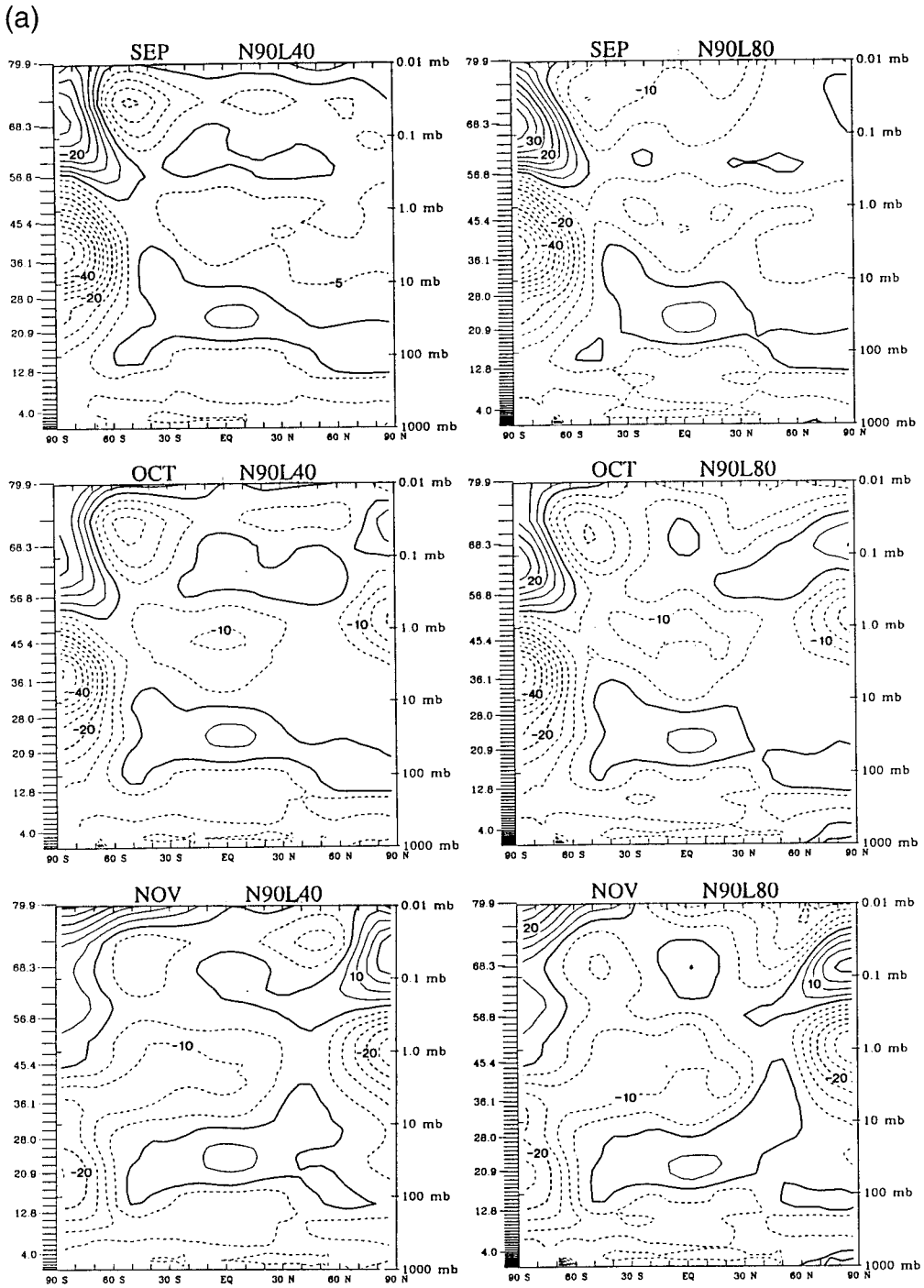

FIG. 9. As in Fig. 4, but for September, October, and November.

equatorial westerly jets in the L80 simulation are also somewhat more narrowly confined near the equator than the easterly jets, again in agreement with observations of the wind structure in the real QBO (Hamilton 1984, 1985; Dunkerton and Delisi 1985).

Preliminary analysis suggests that the equatorial mean flow accelerations in the stratosphere in the L80 SKYHI simulations are forced by interactions with vertically propagating waves. This is, of course, the driving invoked in the standard theories for the QBO (Lindzen and Holton 1968; Holton and Lindzen 1972; Dunkerton 1997). One surprising aspect of the perpetual equinox simulation is the appearance of up to five alternating easterly and westerly jets stacked on the equator above

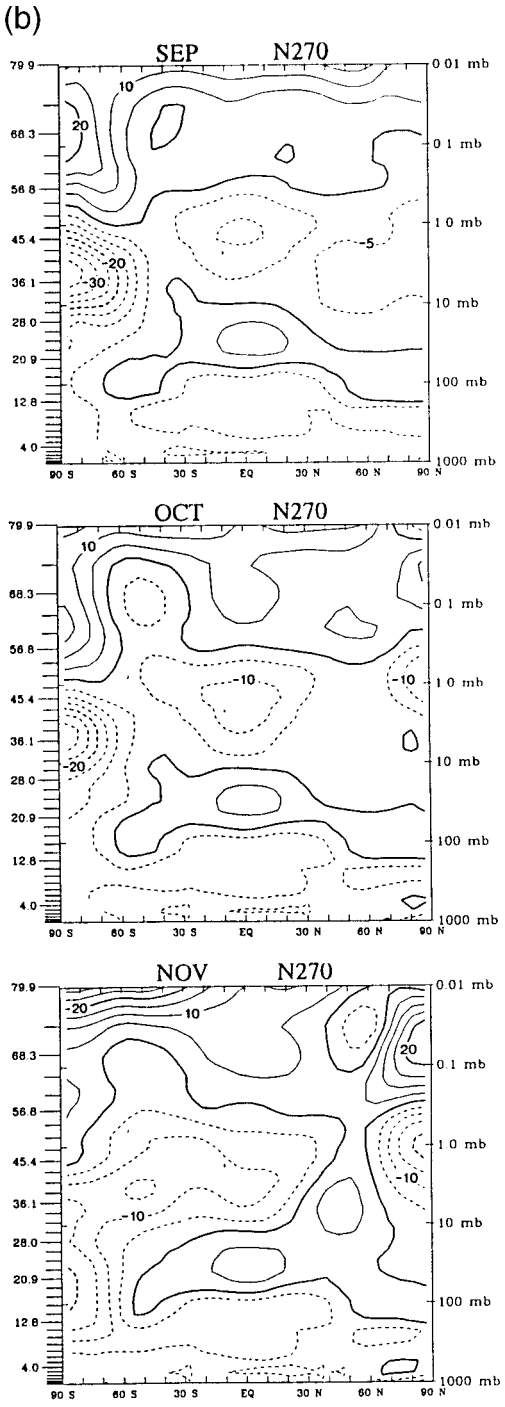

FIG. 9. (*Continued*)

the tropopause. With only forcing from vertically propagating waves, the original Holton–Lindzen (1972) model of equatorial wave–mean flow interaction will predict that at any time there should be at most three alternating mean flow jets appearing above the equator. This seems also to apply to the generalization of the Holton–Lindzen model to include a broad spectrum of

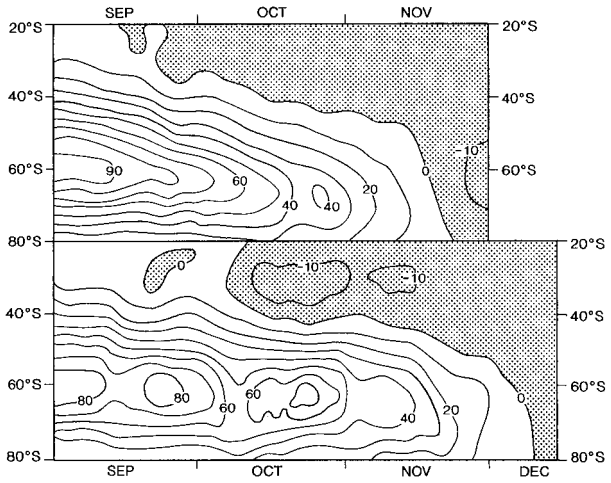

FIG. 10. Evolution of the zonal-mean zonal wind in springtime over the 20°–80°S latitude band at 10 mb. The top is a composite of several years from observations (adapted from Farrara and Mechoso 1986). The bottom is the single realization of the N270L40 SKYHI integration. The contour interval is 10 m s^{-1} and regions of easterlies are shaded.

(noninteracting) waves (Saravanan 1990). Of course, if other mean flow forcing mechanisms are added to the simple Holton–Lindzen model, there is a possibility of more complicated mean flow structures. Thus, it is less surprising to find multiple jets stacked on the equator in the full seasonally varying SKYHI simulation, where the jets in the mesosphere vary semiannually and are likely forced to some extent by cross-equatorial advection by the mean meridional circulation. Recently Mayr et al. (1997) performed a perpetual equinox simulation with a zonally averaged model of the circulation up to the lower thermosphere. The eddy forcing of the mean flow in this model came from a spectrum of gravity waves as parameterized by the Hines (1997) scheme. Their results for the equatorial zonal-mean zonal wind show a downward-propagating QBO-like oscillation with multiple jets similar to those seen in the present

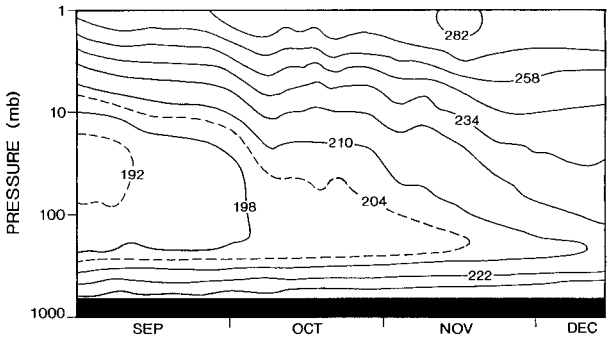

FIG. 11. Evolution of the springtime zonal-mean temperature averaged between 70° and 80°S in the N270L40 SKYHI integration. Contours are labelled in K and the interval between solid contours is 12°. In addition to the solid contours two intermediate contours are plotted for the 192 and 204 K values.

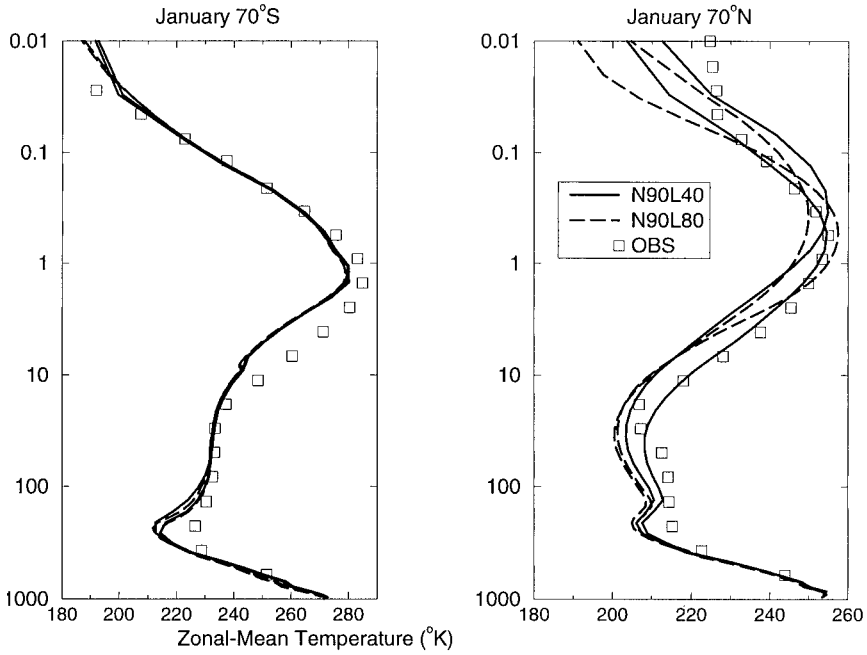

FIG. 12. Zonal-mean zonal temperature in January N90L40 and N90L80 models at 70°S (left) and 70°N (right) and the observed climatology of Fleming et al. (1988).

SKYHI GCM simulation. The Hines parameterization allows parts of the wave spectrum to break nonlinearly (in contrast to the Holton–Lindzen or Saravanan models), and it is possible that this allows for the richer behavior of the equatorial winds in the Mayr et al. model. However, it should also be noted that some three-dimensional GCMs have incorporated versions of the Hines scheme (e.g., Manzini et al. 1997; McFarlane et al. 1997) and thus far none of these models has exhibited a significant tropical mean-flow oscillation. The dynamics underlying occurrence of the large number of jets in the present perpetual equinox GCM experiment is now under investigation.

5. Discussion

This paper has described some basic aspects of the climate simulations obtained with versions of a troposphere–stratosphere–mesosphere GCM run at unprecedentedly high horizontal and vertical resolutions. The results indicate that there is strong sensitivity of the global-scale stratospheric circulation to the model resolution even as horizontal grid spacings are reduced to ~30 km or vertical grid spacings are reduced to ~400 m. Increasing either the horizontal or vertical resolution in the model leads to improvements in the overall middle-atmospheric simulation. The sensitivity of the model performance to resolution differs very much between Tropics and extratropics, however. The extratropical middle-atmospheric simulation seems to be relatively insensitive to increases in vertical resolution beyond the L40 standard but is very sensitive to horizontal resolution. Even with N90 horizontal grid spacing, the SH early winter polar temperatures in the upper stratosphere are 30°C or more lower than observed and the SH polar night jet is significantly stronger than observed. At N270 resolution the bias in SH polar temperatures is reduced to ~10° in early winter and the SH polar night jet looks quite realistic. Later in the winter the simulation deviates somewhat further from observations, but it appears that the N270 SKYHI is the first model to get reasonably close to the goal of a realistic self-consistent simulation of the seasonal evolution of the SH stratospheric circulation, without parameterized wave drag.

The zonal-mean zonal winds and temperatures in the troposphere appear to be significantly less sensitive to the changes in model resolution considered here (although the midlatitude surface westerlies in the winter hemisphere are stronger at N270 than N90 resolution; see also Jones et al. 1997). The dependence of tropospheric simulation on horizontal resolution in GCMs has been examined by, for example, Boer and Lazare (1988), Boyle (1993), and Held and Suarez (1994). None of these studies have considered the very high resolution employed in the present SKYHI runs, but the indication in these earlier papers is that the global-scale features of the tropospheric climatology have largely (if not completely) converged when model grid spacing is reduced below a few hundred kilometers. The very different experience for the middle atmosphere documented here is presumably due to the much greater influence of gravity waves on the large-scale middle-atmospheric circulation.

The tropical stratospheric circulation in the SKYHI

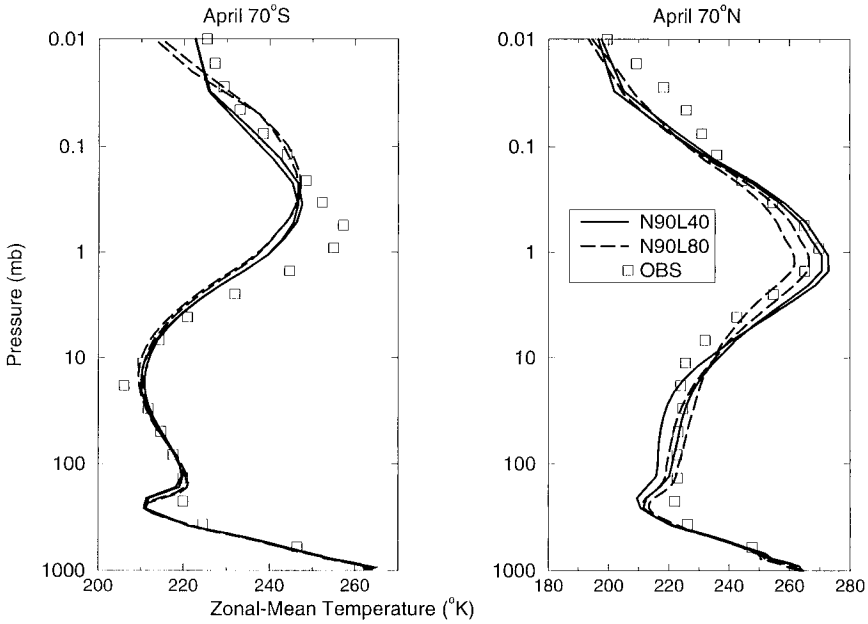

FIG. 13. As in Fig. 12, but for April.

simulations shows a remarkable dependence on vertical resolution. The N90L40 model has virtually no variation in the equatorial lower-stratospheric winds, but the N90L80 model has a long-period oscillation with peak-to-peak amplitude ~50 m s^{-1}, and that is characterized by downward propagation of wind reversals similar to that seen in the QBO. This overall behavior appears to be consistent with recent results from spectral GCMs reported by Takahashi (1996) and Horinouchi and Yoden (1998). However, it is important to note that not all GCMs produce QBO-like oscillations when vertical grid spacing is reduced to ~700 m. Hamilton and Yuan (1992) integrated a version of the GFDL spectral climate model with ~700-m vertical grid spacing throughout the stratosphere and obtained no indication of any significant evolution of the tropical zonal-mean zonal winds. Boville and Randel (1992) found no equatorial mean wind oscillation in their T21 version of the NCAR GCM even with ~700-m vertical grid spacing. Takahashi (1996) also notes that in its standard formulation the CCSR GCM does not produce a QBO-like oscillation even with high vertical resolution. In order to for the CCSR model to oscillate, both the standard subgrid-scale horizontal diffusion and the standard moist convection scheme must be changed.

The present results may have some relevance to the issue of appropriate ratios of horizontal-to-vertical grid spacing in GCMs. One standard sometimes advocated is to require the ratio of the horizontal-to-vertical grid spacing to be equal to the Brunt–Väisälä frequency divided by Coriolis parameter, N/f. For typical midlatitude conditions $N/f \sim 100$ in the troposphere and ~200 in the stratosphere. For the upper-tropospheric–lower-stratosphere region the horizontal-to-vertical grid spacing ratio, $\Delta x/\Delta z$, in the present N30L40 model is ~200; for N90L40 $\Delta x/\Delta z \sim 75$, for N90L80 $\Delta x/\Delta z \sim 150$, for N90L160 $\Delta x/\Delta z \sim 300$, and for N270L40 $\Delta x/\Delta z \sim 25$. The extratropical stratospheric simulation obtained with SKYHI appears to be much more sensitive to Δx rather than the $\Delta x/\Delta z$ ratio. The results discussed here suggest that the key to improving the stratospheric simulation over the N90L40 baseline case is decreasing Δx, rather than increasing the $\Delta x/\Delta z$ ratio by reducing Δz. It is interesting to note that limited-area numerical simulation models have frequently used $\Delta x/\Delta z$ values considerably smaller than the typical midlatitude N/f (e.g., Mailhot et al. 1997). Indeed, cloud-resolving mesoscale models are often run with $\Delta x/\Delta z \sim 5$ (e.g., Alexander et al. 1995). Lindzen and Fox-Rabinovitz (1989) advocated very large $\Delta x/\Delta z$ ratios (of the order of 10^3–10^4) for models that include the equatorial region (necessary in their view for an adequate representation of vertically propagating internal waves). The indication from the present SKYHI results is that the lack of a QBO in simulations cannot be attributed simply to the $\Delta x/\Delta z$ ratio employed. The key to obtaining a QBO-like oscillation appears to be the use of a sufficiently small Δz rather than a large $\Delta x/\Delta z$ ratio.

The very fine resolution models discussed here are obviously not now practical for long chemistry and climate simulations. However, much can be learned through examination of the results of the high-resolution models and further analysis is now under way. In particular, the details of the model gravity wave field and its dependence on both horizontal and vertical resolution are being studied. The behavior of the tropical mean winds is now being investigated in versions of SKYHI with different spatial resolutions and different scaling

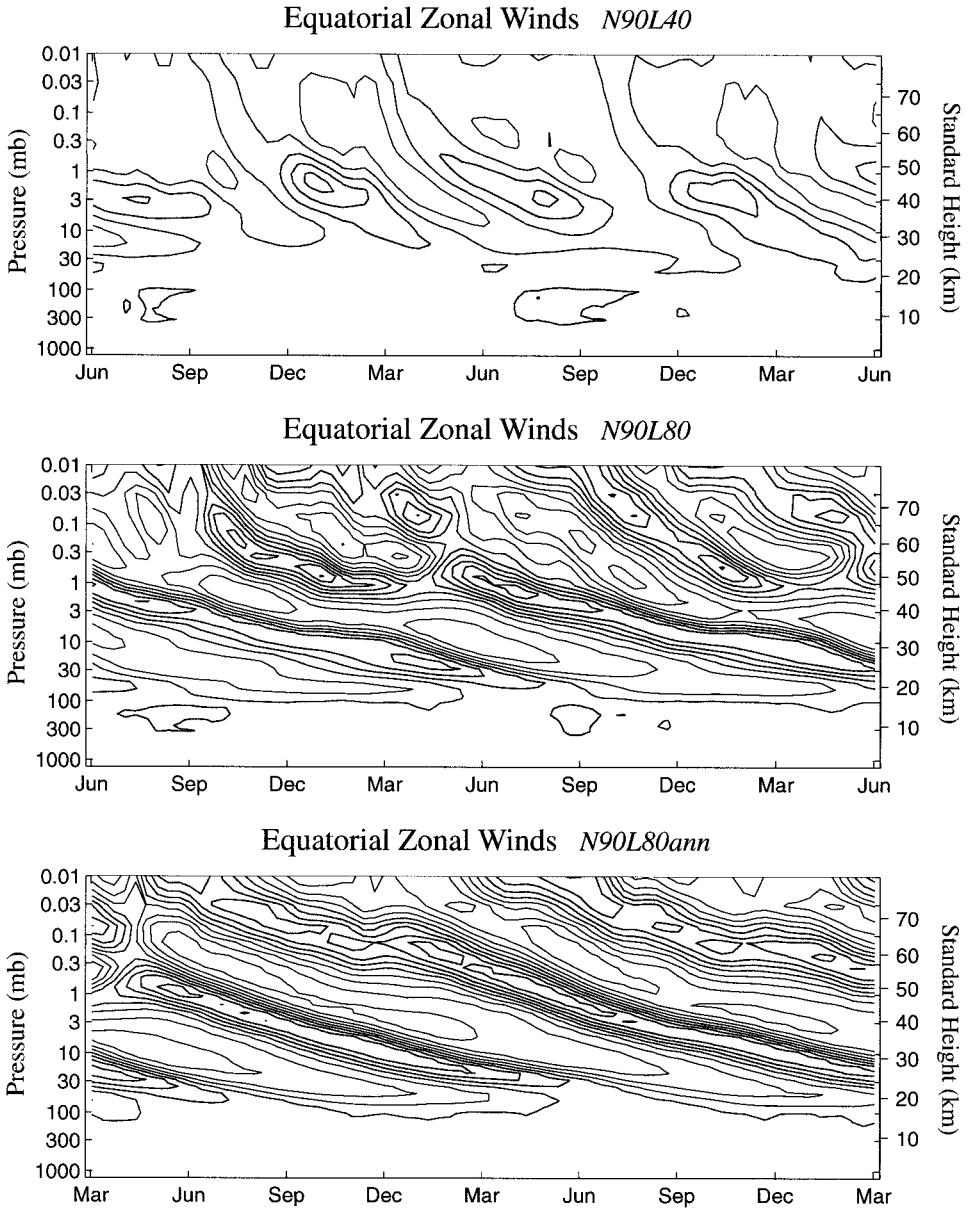

FIG. 14. The height–time evolution of the equatorial zonal-mean wind in various SKHYI integrations. (top) The N90L40 control integration. (middle) The N90L80 control integration. (bottom) The N90L80 perpetual equinox integration. The contour interval is 10 m s^{-1} and easterlies are shaded.

of subgrid-scale dissipation parameterizations. Aspects of the high-resolution control simulations in the troposphere are also being examined. Koshyk et al. (1999) have found that the horizontal spectrum of kinetic energy in the troposphere of the N270 simulation agrees rather well with available observations (e.g., Nastrom and Gage 1985). Hamilton and Hemler (1997) showed that the N270 simulation included tropical cyclones of quite realistic intensity, structure, and development. Other aspects of the synoptic meteorology of the high-resolution SKYHI runs (including some, such as upper-tropospheric fronts, that might be more affected by limited vertical resolution) will be investigated.

There is no definitive indication in the present results that the global-scale simulations have converged, even at the highest resolution considered. It is even possible that aspects of the simulation may get worse as still finer resolution is employed. Thus, as computer resources allow, it is planned to attempt even higher-resolution simulations with the SKYHI model. A version combining the N270 horizontal resolution with significantly enhanced vertical resolution is an obvious case

of interest. Further refinement of the horizontal resolution may also be attempted, although the restriction of the current SKHYI code to hydrostatic motions may then become a significant limitation.

Acknowledgments. The authors wish to thank Jerry Mahlman for his interest in this project and his comments on the manuscript. Phil Jones and Chris Kerr contributed to coding the model so that it can run efficiently on massively parallel computers. Dan Schwarzkopf assisted with the implementation of the radiation codes. The $0.6° \times 0.72°$ model integrations were performed by Phil Jones at Los Alamos National Laboratory. Some of the 160-level model integration was performed on the Cray T3E computer of the National Energy Research Scientific Computer Division, which is supported by the Office of Energy Research of the U.S. Department of Energy under Contract DE-AC03-76SF00098.

REFERENCES

Alexander, M. J., J. R. Holton, and D. R. Durran, 1995: The gravity wave response above deep convection in a squall line simulation. *J. Atmos. Sci.,* **52,** 2212–2236.

Andrews, D. G., J. D. Mahlman, and R. W. Sinclair, 1983: Eliassen–Palm diagnostics of wave-mean flow interaction in the GFDL ''SKYHI'' general circulation model. *J. Atmos. Sci.,* **40,** 2768–2784.

——, J. R. Holton, and C. B. Leovy, 1987: *Middle Atmosphere Dynamics.* Academic Press, 489 pp.

Barnett, J. J., and M. Corney, 1985: Middle atmosphere reference model derived from satellite data. *Middle Atmosphere Program Handbook,* Vol. 16, 47–85.

Belmont, A. D., D. G. Dartt, and G. D. Nastrom, 1974: Periodic variations in stratospheric zonal wind from 20 to 65 km at 80°N to 70°S. *Quart. J. Roy. Meteor. Soc.,* **100,** 203–211.

Boer, G. J., and M. Lazare, 1988: Some results concerning the effect of horizontal resolution and gravity-wave drag on simulated climate. *J. Climate,* **1,** 789–806.

Boville, B. A., 1991: Sensitivity of the simulated climate to model resolution. *J. Climate,* **4,** 469–485.

——, 1995: Middle atmosphere version of CCM2 (MACCM2): Annual cycle and interannual variability. *J. Geophys. Res.,* **100,** 9017–9039.

——, and W. J. Randel, 1992: Equatorial waves in a stratospheric GCM: Effects of vertical resolution. *J. Atmos. Sci.,* **49,** 785–801.

Boyle, J. S., 1993: Sensitivity of dynamical quantities to horizontal resolution for a climate simulation using the ECMWF (Cycle 33) model. *J. Climate,* **6,** 796–815.

Dunkerton, T. J., 1997: The role of gravity waves in the quasibiennial oscillation. *J. Geophys. Res.,* **102,** 26 053–26 076.

——, and D. Delisi, 1985: Climatology of the equatorial lower stratosphere. *J. Atmos. Sci.,* **42,** 1199–1208.

Farrara, J. D., and C. R. Mechoso, 1986: Observational study of the final warming in the Southern Hemisphere stratosphere. *Geophys. Res. Lett.,* **13,** 1232–1235.

Fels, S. B., and M. D. Schwarzkopf, 1981: An efficient, accurate algorithm for calculating an efficient, accurate algorithm for calculating CO_2 15 micron band cooling rates. *J. Geophys. Res.,* **86,** 1205–1232.

——, J. D. Mahlman, M. D. Schwarzkopf, and R. W. Sinclair, 1980: Stratospheric sensitivity to perturbations in ozone and carbon dioxide: Radiative and dynamical responses. *J. Atmos. Sci.,* **37,** 2265–2297.

Fleming, E. L., S. Chandra, M. R. Schoeberl, and J. J. Barnett, 1988: Monthly mean global climatology of temperature, wind, geopotential height, and pressure for 0–120 km. NASA Tech. Memo. 100697, 85 pp. [Available from NASA/Goddard Space Flight Center, Greenbelt, MD 20771.]

Hamilton, K., 1984: Mean wind evolution through the quasi-biennial cycle in the tropical lower stratosphere. *J. Atmos. Sci.,* **41,** 2113–2125.

——, 1985: The initial westerly acceleration phase of the stratospheric quasi-biennial oscillation as revealed in FGGE analyses. *Atmos.–Ocean.,* **23,** 188–192.

——, 1995: Comprehensive modelling of middle atmospheric climate: Some recent results. *Climate Dyn.,* **11,** 223–241.

——, 1996: Comprehensive meteorological modelling of the middle atmosphere: A tutorial review. *J. Atmos. Terr. Phys.,* **58,** 1591–1628.

——, 1997: The role of parameterized drag in a troposphere-stratosphere-mesosphere general circulation model. *Gravity Wave Processes—Their Parameterization in Global Climate Models,* K. Hamilton, Ed., Springer-Verlag, 337–350.

——, and L. Yuan, 1992: Experiments on tropical stratospheric mean wind variations in a spectral general circulation model. *J. Atmos. Sci.,* **49,** 2464–2483.

——, and R. S. Hemler, 1997: Appearance of a super-typhoon in a global climate model simulation. *Bull. Amer. Meteor. Soc.,* **78,** 2874–2876.

——, R. J. Wilson, J. D. Mahlman, and L. J. Umscheid, 1995: Climatology of the SKYHI troposphere-stratosphere-mesosphere general circulation model. *J. Atmos. Sci.,* **52,** 5–43.

Haynes, P. H., C. J. Marks, M. E. McIntyre, T. G. Shepherd, and K. P. Shine, 1991: On the ''downward control'' of extratropical diabatic circulations by eddy-induced mean zonal forces. *J. Atmos. Sci.,* **48,** 651–678.

Held, I. M., and M. J. Suarez, 1994: A proposal for the intercomparison of the dynamical cores of atmospheric general circulation models. *Bull. Amer. Meteor. Soc.,* **75,** 1825–1830.

Hines, C. O., 1997: Doppler-spread parameterization of gravity-wave momentum deposition in the middle atmosphere. Part I: Basic formulation. *J. Atmos. Solar-Terr. Phys.,* **59,** 371–386.

Holton, J. R., and R. S. Lindzen, 1972: An updated theory for the quasi-biennial cycle of the tropical stratosphere. *J. Atmos. Sci.,* **29,** 1076–1080.

Horinouchi, T., and S. Yoden, 1998: Wave-mean flow interaction associated with a QBO-like oscillation simulated in a simplified GCM. *J. Atmos. Sci.,* **55,** 502–526.

Jones, P. W., K. Hamilton, and R. J. Wilson, 1997: A very high-resolution general circulation model simulation of the global circulation in Austral winter. *J. Atmos. Sci.,* **54,** 1107–1116.

Koshyk, J. N., K. Hamilton, and J. D. Mahlman, 1999: Simulation of the $k^{-5/3}$ mesoscale spectral regime in the GFDL SKYHI middle atmosphere general circulation model. *Geophys. Res. Lett.,* **26,** 843–846.

Levy, H., J. D. Mahlman, and W. J. Moxim, 1982: Tropospheric N_2O variability. *J. Geophys. Res.,* **87,** 3061–3080.

Lindzen, R. S., and J. R. Holton, 1968: A theory of the quasi-biennial oscillation. *J. Atmos. Sci.,* **25,** 1095–1107.

——, and M. Fox-Rabinovitz, 1989: Consistent vertical and horizontal resolution. *Mon. Wea. Rev.,* **117,** 2575–2583.

McFarlane, N. A., C. McLandress, and S. Beagley, 1997: Seasonal simulations with the Canadian Middle Atmosphere Model: Sensitivity to the Doppler-spread gravity wave parametrization. *Gravity Wave Processes—Their Parameterization in Global Climate Models,* K. Hamilton, Ed., Springer-Verlag, 351–366.

Mahlman, J. D., and L. J. Umscheid, 1987: Comprehensive modeling of the middle atmosphere: The influence of horizontal resolution. *Transport Processes in the Middle Atmosphere,* G. Visconti and R. Garcia, Eds., D. Reidel, 251–266.

——, J. P. Pinto, and L. J. Umscheid, 1994: Transport, radiative, and dynamical effects of the Antarctic ozone hole: A GFDL ''SKYHI'' model experiment. *J. Atmos. Sci.,* **51,** 489–508.

Mailhot, J., R. Sarrazin, B. Bilodeau, N. Brunet, and G. Pellerin, 1997: Development of the 35-km version of the Canadian regional forecast system. *Atmos.–Ocean*, **35,** 1–28.

Manzini, E., N. A. McFarlane, and C. McLandress, 1997: Middle atmosphere simulations with the ECHAM4 model: Sensitivity to the Doppler-spread gravity wave parameterization. *Gravity Wave Processes—Their Parameterization in Global Climate Models*, K. Hamilton, Ed., Springer-Verlag, 367–381.

Mayr, H. G., J. G. Mengel, C. O. Hines, K. L. Chan, N. F. Arnold, C. A. Reddy, and H. S. Porter, 1997: The gravity wave Doppler spread theory applied in a numerical spectral model of the middle atmosphere. Part 2: Equatorial oscillations. *J. Geophys. Res.*, **102,** 26 093–26 015.

Medvedev, A. S., G. P. Klassen, and S. R. Beagley, 1998: On the role of an anisotropic gravity wave spectrum in maintaining the circulation of the middle atmosphere. *Geophys. Res. Lett.,* **25,** 509–512.

Nastrom, G. D., and K. Gage, 1985: Climatology of atmospheric wavenumber spectra of wind and temperature observed by commercial aircraft. *J. Atmos. Sci.,* **42,** 950–960.

Naujokat, B., 1986: An update of the observed quasi-biennial oscillation of the stratospheric winds over the tropics. *J. Atmos. Sci.*, **43,** 1873–1877.

Newell, R. E., J. W. Kidson, D. G. Vincent, and G. J. Boer, 1974: *The General Circulation of the Tropical Atmosphere and Interactions with Extratropical Latitudes.* The MIT Press, 371 pp.

Orris, R. L., 1997: Ozone and temperature: A test of the consistency of models and observations in the middle atmosphere. Ph.D. thesis, Princeton University, Princeton, NJ, 240 pp.

Randel, W. J., 1992: Global atmospheric circulation statistics, 1000-1 mb. NCAR Tech. Note TN-366+STR, 256 pp. [Available from Publications Office, National Center for Atmospheric Research, P.O. Box 3000, Boulder, CO 80307.]

Saravanan, R., 1990: A multiwave model of the quasi-biennial oscillation. *J. Atmos. Sci.*, **47,** 2465–2474.

Takahashi, M., 1996: Simulation of the stratospheric quasi-biennial oscillation using a general circulation model. *Geophys. Res. Lett.*, **23,** 661–664.

Wu, M. F., M. A. Geller, E. R. Nash, and M. E. Gelman, 1987: Global atmospheric circulation statistics—Four year averages. NASA Tech. Memo. 100690, 70 pp. [Available from NASA/Goddard Space Flight Center, Greenbelt, MD 20771.]